

MASTER

conf -
790125--44

THE INCLUSION OF MOBILE HELIUM IN A RATE THEORY MODEL OF VOID SWELLING*

M. H. Yoo and L. K. Mansur

Metals and Ceramics Division, Oak Ridge National Laboratory, Oak Ridge, Tennessee 37830 USA

The effect of mobile helium on swelling has been studied by using a rate theory model of void growth. The partitioning of mobile helium to various internal sinks and the trapping of interstitial helium atoms by vacancies were included in the model. Helium gas generated during neutron irradiation increases swelling at temperatures above the peak void swelling temperature. Two temperature regimes of enhanced swelling are related to gas-assisted void growth and gas-driven bubble growth. Swelling due to void and bubble growth in a fusion reactor first wall is predicted using nickel as an example, and the effects of dislocation density and grain size on swelling are discussed. It is found that, as compared to simultaneous helium injection during heavy-ion bombardment, the method of helium preinjection is inadequate in simulating a fusion reactor condition.

1. INTRODUCTION

It is generally believed that helium created by α -particle-producing transmutations during neutron irradiation may have significant effects on the deformation behavior of a fusion reactor first wall material, such as void swelling, surface blistering, and intergranular fracture. The present paper considers the effect of helium on void swelling from a theoretical point of view.

The effect of mobile helium on void nucleation during irradiation has been treated by Hall and Wiedersich [1] and Hall [2]. By including into a steady-state void nucleation model the trapping and detrapping of helium and the helium emission from voids containing helium gas, they [1] found that the void nucleation rate in nickel at temperatures above 500°C is enhanced significantly at the displacement damage rate of 10^{-5} dpa/s. Hayns et al. [3,4] have investigated the effect of helium on void growth by considering simultaneous heavy-ion damage and helium injection, and concluded that the high-temperature "second peak" which is a significant feature of the void swelling in neutron-irradiated type 316 stainless steel can be correlated quantitatively with the dual-beam simulation experimental situations.

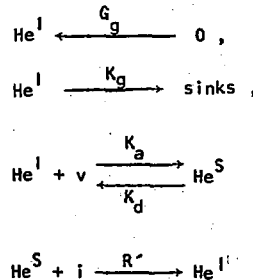
The purpose of the present paper is two-fold; (a) to develop rate equations for cavity (void or bubble) growth in irradiated materials that include the role of mobile helium, and (b) to predict the effects of mobile helium on swelling in a fusion reactor first wall, a heavy-ion damage experimental situation with simultaneous helium injection, and a neutron irradiation

*Research sponsored by the Materials Sciences Division, U.S. Department of Energy under contract W-7405-eng-26 with the Union Carbide Corporation.

experimental situation in a mixed neutron spectrum fission reactor. A sample calculation will be made on nickel, and the calculated results on helium effects will be discussed in comparison to published data.

2. RATE EQUATIONS

To include mobile helium in the reaction rate theory of void swelling [5-8], the following reactions are considered:



where He^I designates those helium gas atoms in the interstitial positions, He^S denotes those in the vacant lattice sites, and v and i denote monovacancies and self-interstitials, respectively. The reaction rate constants are; G_g , the generation rate of He^I ; K_g , diffusional loss rate of He^I to unsaturable sinks* (dislocations, voids or bubbles, and grain boundaries); K_a , trapping of He^I by v to form a He^S ; K_d , thermal

*This is an approximation for the present time since any internal sink has a saturation limit.

NOTICE

This report was prepared as an account of work sponsored by the United States Government. Neither the United States nor the United States Department of Energy, nor any of their employees, nor any of their contractors, subcontractors, or their employees, makes any warranty, express or implied, or assumes any legal liability or responsibility for the accuracy, completeness or usefulness of any information, apparatus, product or process disclosed, or represents that its use would not infringe privately owned rights.

DISTRIBUTION OF THIS DOCUMENT IS UNLIMITED

By acceptance of this article, the publisher or recipient acknowledges the U.S. Government's right to retain a nonexclusive, royalty-free license in and to any copyright covering the article.

leg

detrapping of He^S; and R^{*} is for the transition of He^S to He^I by encountering an i. In the present model, therefore, helium gas atoms are created at a prescribed rate, and they migrate to the internal sinks. The reaction of interstitial helium with a vacancy is fully taken into account, but that with a self-interstitial is not considered in this paper.

The rate equations that include these reactions are:

$$\dot{C}_v = G_v - RC_v C_i - K_v C_v - K_a C_v C_g + K_d C_{vg}, \quad (1)$$

$$\dot{C}_i = G_i - RC_v C_i - K_i C_i - R^* C_i C_{vg}, \quad (2)$$

$$\dot{R}_v = [D_v(C_v - C_v^V) - D_i C_i] / R_v, \quad (3)$$

$$\dot{C}_g = G_g - K_g C_g - K_a C_v C_g + K_d C_{vg} + R^* C_i C_{vg}, \quad (4)$$

$$\dot{C}_{vg} = K_a C_v C_g - K_d C_{vg} - R^* C_i C_{vg}, \quad (5)$$

$$\dot{n}_g = 4\pi R_v D_g C_g / \Omega, \quad (6)$$

where C's are the average defect concentration in atom fraction, R_v the radius of a cavity (void or bubble), and n_g is the number of helium gas atoms in a cavity. The subscripts v, i, V, g, and vg denote vacancies, interstitials, cavities, mobile helium atoms, and trapped substitutional helium atoms, respectively. G_α is the defect generation rate,* and Ω is the atomic volume.

The total sink strength for α = v, i, or g mobile defects is taken as [9]

$$S_\alpha = k_\alpha^2 = Z_\alpha L + 4\pi R_v N_v + \frac{6}{d} (Z_\alpha L + 4\pi R_v N_v)^{1/2}, \quad (7)$$

where L and N_v are the dislocation and void number densities, and d is the grain size. While cavities and grain boundaries are treated as neutral sinks for all three types of mobile defects, the capture efficiency of dislocations is given by Z_α = 2π/ln(R_L/r_α^D) with the outer cut-off radius, R_L = (πL)^{-1/2}, and the effective capture radius of a dislocation for the defects of α type, r_α^D = r_c(1 + δ_α^D) [5,6]. r_c is an inner cut-off core radius and δ_α^D is the preference factor [5,6].

*This accounts for the thermal emission of vacancies from the internal sinks and the vacancy fraction involved in the athermal nucleation of vacancy clusters in displacement damage cascades, and also the implanted extra self-interstitials in the case of self-ion damage.

3. DEFECT PARAMETERS

The reaction rate constants in Eqs. (1-6) are related to various parameters of point defects. The defect loss rate to the internal sinks is K_α = D_αS_α, where D_α is the diffusion constant of α type defects. The recombination rate constants are R = 4πr₀(D_i + D_v)/Ω and R* = 4πr₀^D/Ω, and the trapping rate constant is K_a = 4πr₀v_g(D_g + D_v)/Ω. It is assumed that r_{vg} = r₀^D = r₀. The detrapping rate constant is K_d = K₀exp[-(E_g^m + E_{vg}^b)/kT], where E_g^m is the migration energy of He^I, E_{vg}^b the bonding energy between He^I and v, and the usual meaning for kT. The attempt frequency term may be approximated [10] by K₀^g = D₀^g/b², where D₀^g is the pre-exponential diffusivity of helium and b is a unit jump distance.

All the defect parameters used in the present work for Ni are listed in Table 1. The defect and sink parameters are the same as those in the previous paper on the role of divacancies [11], and the parameters for helium are from Baskes and Wilson [12].

Table 1. Input Parameters for Nickel

Defect Parameters	Material Constants	Sink Parameters
S _v ^f = 1.5 k	a ₀ = 0.35 nm	d = 30 μm
E _v ^f = 1.39 eV		2lnN _v = ∑ _{z=0} ⁴ A _z T ²
D _v ⁰ = 1.6 × 10 ⁻² cm ² /s	r ₀ = 8.38 a ₀ T ^{-1/3}	2lnL = ∑ _{z=0} ⁴ A _z T ²
E _v ^m = 1.38 eV		δ _i ^D = 0.6
D _i ⁰ = 0.8 × 10 ⁻² cm ² /s	Γ = 1000 mJ/m ²	δ _g ^D = 0.3
E _i ⁰ = 0.15 eV		δ _v ^D = 0.0
D _g ⁰ = 1 × 10 ⁻² cm ² /s		
E _g ⁰ = 0.2 eV		
E _{vg} ⁰ = 3.16 eV		
	N _v	L
	A ₀ 31.43	22.81
	A ₁ 2.47 × 10 ⁻²	1.46 × 10 ⁻³
	A ₂ -5.78 × 10 ⁻⁵	-6.66 × 10 ⁻⁶
	A ₃ 5.94 × 10 ⁻⁸	9.36 × 10 ⁻⁹
	A ₄ -2.50 × 10 ⁻¹¹	-6.61 × 10 ⁻¹²

4. FUSION REACTOR MATERIALS

Using a fusion reactor first wall neutron spectrum under a neutron wall loading of 1 MW/m², Gabriel et al. [13] have computed G = 3.89 × 10⁻⁶ dpa/s and G_g = 1.3 × 10⁻⁵ appm/s for Ni. The rate equations (1-6) were integrated by use of the numerical method developed earlier [6]. The calculated swelling of Ni after 10 dpa is shown in Fig. 1. The effect of mobile helium generated during neutron irradiation on swelling is to increase swelling at high temperatures above the peak swelling temperature. The curve (a) is obtained when all the helium generated is assumed to be absorbed into voids as was treated by Hayns et al. [3]. The curve (b) is obtained when the population of mobile helium is

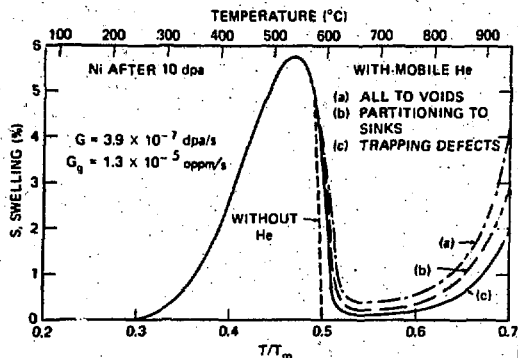


Fig. 1. The effect of mobile helium on swelling of Ni under a fusion reactor first-wall condition.

partitioned into dislocations, cavities, and grain boundaries in proportion to the relative sink strength. The curve (c) results when helium-vacancy trapping is taken into account in addition to the helium partitioning.

Assuming the van der Waals gas law is applicable to those helium containing cavities, one may express for the internal gas pressure as

$$p_g = n_g kT / \left(\frac{4}{3} \pi R^3 - n_g B \right), \quad (8)$$

where B is the van der Waals coefficient. A dimensionless parameter useful in the present analysis is $\eta = 2\Gamma/p_g R\gamma$, where Γ is the void specific surface energy. A cavity is a void, an equilibrium bubble, or an "overpressurized" bubble depending on whether $\eta > 1$, $\eta = 1$, or $\eta < 1$. Another useful parameter is "bubble character," which may be defined as the ratio of the actual number of gas atoms in a cavity to the number of gas atoms required for an equilibrium bubble of the same size. "Bubble character" and the parameter η are plotted against temperature in Fig. 2(a) together with the curve (c) of Fig. 1 shown again in Fig. 2(b). Void swelling is bias-driven at 230–550°C and gas-assisted at 550–780°C. Beyond the transition from voids to bubbles, $T > 780^\circ\text{C}$, swelling is due to gas-driven bubble growth.

In order to study the change in swelling in response to microstructural variation two separate calculations were made, one by varying dislocation density and the other by varying grain size; the calculated results are shown in Fig. 3. In the temperature regime of bias-driven swelling the increase in dislocation sink strength enhances swelling by increasing the net flux of

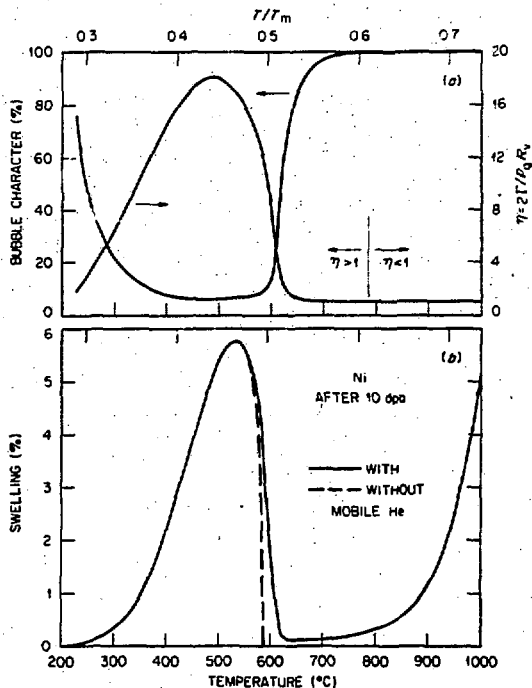


Fig. 2. (a) Bubble character and (b) the effect of helium on swelling.

vacancies to voids,* whereas in the gas-driven swelling it reduces swelling since dislocations remove gas atoms which would otherwise pressurize bubbles. The decrease in grain size increases the relative sink strength of neutral grain boundaries — see Eq. (7), which should cause a swelling reduction at all temperatures. The calculated results shown in Fig. 3 are consistent with the expected response of swelling discussed above. Figure 3 indicates that the gas-driven swelling may be suppressed almost entirely by refining the grain size to 5 μm if the integrity of such a fine-grain polycrystal is maintained.

5. SIMULATION CONDITIONS

A heavy-ion damage condition, as a simulation of the neutron irradiation of the first wall discussed in the previous section, was considered

*This is the case for the relative sink strengths presently considered. In other cases, for example, where dislocations are the dominant sinks and recombination is minor, an increase in dislocation density will decrease swelling [7].

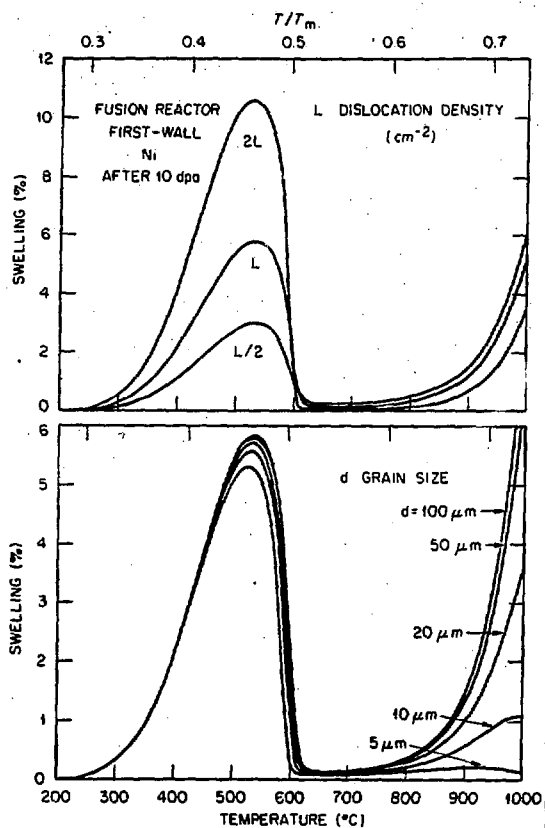


Fig. 3. The effects of dislocation density and grain size on swelling.

by increasing both the dose rate and the gas production rate by 10^{-4} to $G = 3.9 \times 10^{-3}$ dpa/s and $G_g = 1.3 \times 10^{-1}$ appm/s. The ratio of the gas production to the displacement damage, 33 appm/dpa, is maintained. The swelling result for this simultaneous helium injection case is shown as dashed curve (a) in Fig. 4. A case for preinjection of 330 appm helium was also considered,* and the swelling in this case is shown as dashed curve (b) in Fig. 4. The solid curves for swelling and bubble character are again for the fusion reactor first wall. The temperature shift of 190°C was found by iteration on the temperature dependent sink densities and the resulting temperature dependent swelling. The simultaneous helium injection causes bubble growth at temperatures above 900°C , giving rise to a swelling characteristics similar to the solid curve. The preinjection of helium, however, does not cause bubble growth at high temperatures. This*

*In the present study, all the preinjected helium were placed initially as interstitial atoms.

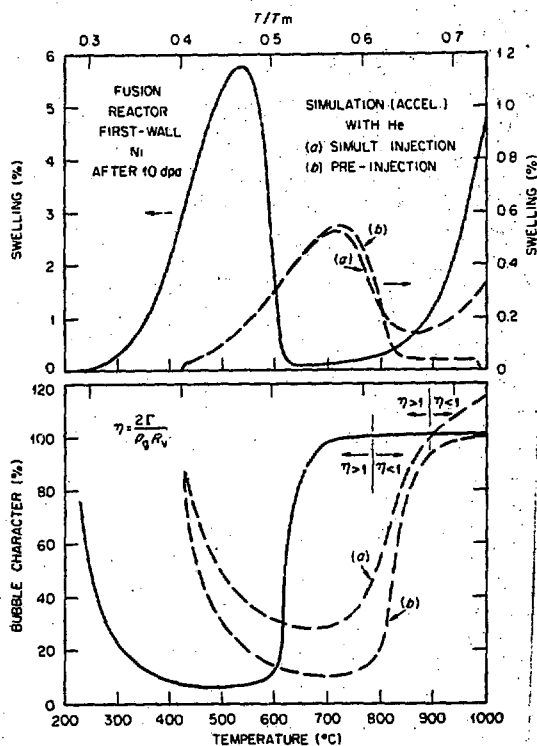


Fig. 4. Simultaneous injection and preinjection of helium during heavy-ion damage in an accelerator.

is because most preinjected helium interstitials are absorbed into dislocations and grain boundaries when voids are still small in the early stage of irradiation, leaving an insufficient amount of helium to effect enhanced swelling at a high dose.

Another useful method for simulating a high production rate of helium during irradiation is the utilization of mixed neutron spectrum fission reactors, such as the High Flux Isotope Reactor (HFIR) [14]. The equation for the production of helium in the peripheral target position of the HFIR given by Wiffen et al. [14] gives the time dependent gas generation rate as

$$G_g(t) = f \times 1.23 \times 10^{-9} [\exp(-9.38 \times 10^{-9}t) - \exp(-1.91 \times 10^{-7}t)] \quad (9)$$

with the atom fraction of ^{58}Ni $f = 0.67$ for Ni and $f = 8.39 \times 10^{-2}$ for type 316 stainless steel. The temperature dependence of swelling for the HFIR situation was calculated with the same sink densities used for the fusion reactor situation,

and the results are shown in Fig. 5. The two curves for type 316 stainless steel show the difference in swelling due to the time dependent gas generation rate by Eq. (9) and a constant rate of helium generation. The swelling in the fusion reactor first wall Ni calculated in Sect. 4 was extended to 40 dpa, and it is shown as a three-dimensional plot in Fig. 6. The swelling appearance for Ni in the HFIR situation shown in Fig. 5 is very much different from that in Fig. 6. This indicates that the helium effect on swelling using HFIR conditions overestimates the actual situation of a conceptual fusion reactor situation discussed in this paper.

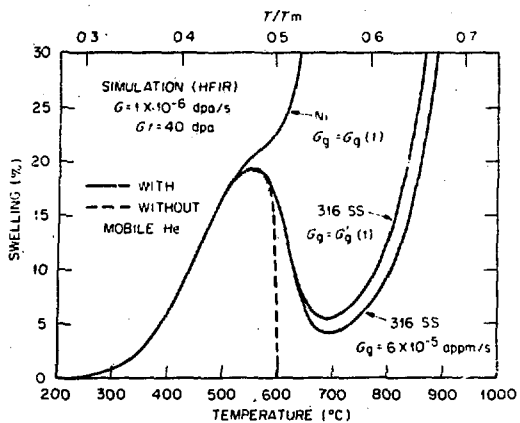


Fig. 5. Simulation of high helium production rate in a fusion reactor by irradiation in HFIR.

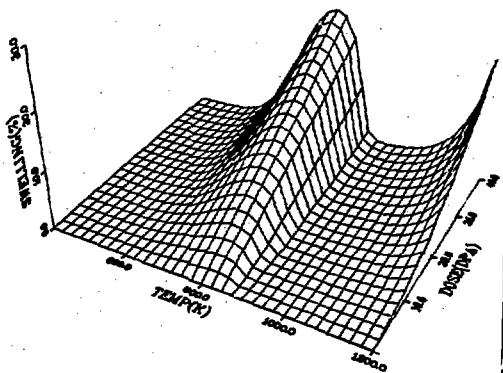


Fig. 6. Temperature and dose dependence of swelling in Ni under a fusion reactor first-wall condition.

6. SUMMARY AND DISCUSSION

In summary, (a) the rate equations for swelling that include the partitioning of mobile helium to dislocation, grain boundaries, and voids and the trapping of interstitial helium atoms by vacancies have been formulated, (b) mobile helium generated during neutron irradiation increases swelling at high temperatures above the peak void swelling temperature, (c) two temperature regimes of enhanced swelling by helium are identified as gas-assisted void growth and gas-driven bubble growth, (d) swelling due to void and bubble growth in a fusion reactor first wall was predicted, and the effect of microstructural variables on swelling was discussed, and (e) the technique of helium pre-injection is inadequate for simulating a fusion reactor condition.

Hayns et al. [3] showed in their Fig. 3 that a small second swelling peak is evident at 500°C near the high temperature cut-off of swelling in type 316 stainless steel even in the absence of helium generation, and that the second peak increases its height as the gas generation rates increase. No indication of a second peak has been detected in the present work. The possible source of this difference in regard to the second swelling peak may be the temperature dependences of sink densities. Hayns et al. [3] used an exponential relation $1/kT$ for sink densities [15], whereas we used the expressions as shown in Table 1, the temperature dependent sink densities, based on the experimental data obtained on Ni by Packan et al. [16].

REFERENCES

- [1] B. O. Hall and H. Wiedersich, in *Radiation Effects in Breeder Reactor Structural Materials* (Proc. Int. Conf. Scottsdale, Ariz.) (1977) 387.
- [2] B. O. Hall, in *Effects of Simultaneous Helium Injection on Void Nucleation in Irradiated Metals* (in this Proceedings).
- [3] M. R. Hayns, M. H. Wood, and R. Bullough, *J. Nucl. Mater.* 75(1978) 241.
- [4] R. Bullough, M. R. Hayns, and M. H. Wood, in *Continuous Gas Generation Effects in Neutron and Simulation Environments* (in this Proceedings).
- [5] M. H. Yoo and L. K. Mansur, *J. Nucl. Mater.* 62(1976) 282.
- [6] M. H. Yoo, *J. Nucl. Mater.* 68(1977) 193.
- [7] L. K. Mansur, *Nucl. Technol.* 40(1978) 3.
- [8] M. H. Yoo, *J. Nucl. Mater.* 79(1979) 135.
- [9] P. T. Heald and J. E. Harbottle, *J. Nucl. Mater.* 67(1977) 229.
- [10] L. K. Mansur and M. H. Yoo, *J. Nucl. Mater.* 67(1977) 229.
- [11] M. H. Yoo, *Philosophical Magazine* (in press).
- [12] M. Baskes and W. D. Wilson, in *Solute Segregation and Phase Stability During Irradiation* (Proc. of Workshop, Gatlinburg, Tenn.) *Journal of Nuclear Materials* (in press).

- [13] T. A. Gabriel, B. L. Bishop, and F. W. Wiffen, Nucl. Technol. 38(1978) 427.
- [14] F. W. Wiffen, E. J. Allen, H. Farrar, IV, E. E. Bloom, T. A. Gabriel, H. T. Kerr, and F. G. Perey, in The Production Rate of Helium during Irradiation of Nickel in Thermal Spectrum Fission Reactors (in this Proceedings).
- [15] M. R. Hayns, private communication.
- [16] N. H. Packan, K. Farrell, and J. O. Stiegler, J. Nucl. Mater. 78(1978) 143.